Available online at www.sciencedirect.com
ScienceDirect
Journal of Sound and Vibration 314 (2008) 571–585
JOURNAL OF SOUND AND VIBRATION
www.elsevier.com/locate/jsvi

Identification of Bouc–Wen hysteretic systems by a hybrid evolutionary algorithm

A.E. Charalampakis, V.K. Koumousis*

Department of Civil Engineering, Institute of Structural Analysis and Aseismic Research, National Technical University of Athens, Athens 15780, Greece

Received 12 July 2007; received in revised form 13 December 2007; accepted 2 January 2008
Handling Editor: C. Morfey
Available online 4 March 2008

Abstract

A new identification method that determines the parameters of Bouc–Wen hysteretic systems is presented. It is based on a hybrid evolutionary algorithm which utilizes selected stochastic operators, heuristics and problem-specific information. The proposed method exhibits efficiency, robustness and insensitivity to noise-corrupted data, while it identifies accurately both hysteretic and viscous damping based on suitable experiments. Its performance is investigated with respect to the information content of the input–output data. The scheme is verified by a hysteretic system representing a full-scale steel cantilever beam which is identified successfully. A series of parametric studies are also conducted that illustrate the inner workings of the proposed method, suggesting appropriate values for the controlling parameters.

1. Introduction

The Bouc–Wen model is a smooth endochronic model that is often used to describe hysteretic phenomena. It was introduced by Bouc [1] and extended by Wen [2], who demonstrated its versatility by producing a variety of hysteretic patterns.

Due to its highly nonlinear nature, identification of Bouc–Wen systems constitutes a challenging problem which has been tackled by a variety of methods, such as Gauss–Newton [3], modified Gauss–Newton [4], Least squares [5], Simplex [6], Levenberg–Marquardt [6,7], extended Kalman filters [6,8], reduced gradient methods [6], Genetic Algorithms (GAs) [9], real-coded GAs [10], Differential Evolution [11,12], adaptive laws [13], etc.

Various techniques have been used to alleviate performance problems. In some methods [4,8,11], the exponential parameter of the model is fixed *a priori* to a specific value. In other cases [3,12], a two-stage scheme is employed which reduces the initial multiplicity of the problem. Approximate initial ranges for the parameter values are determined prior to identification on the basis of phenomenological reasoning [9]. Certain system parameters, most commonly stiffness and viscous damping, are generally considered known.

*Corresponding author. Tel.: +30 2107721657; fax: +30 2107721651.
E-mail address: vkoum@central.ntua.gr (V.K. Koumousis).

0022-460X/$ - see front matter © 2008 Elsevier Ltd. All rights reserved.
doi:10.1016/j.jsv.2008.01.018

In certain dynamical systems, frequency-independent hysteretic damping coexists with viscous damping which may become significant under high velocities [7]. Thus, in these cases, both hysteretic and viscous damping characteristics need to be identified simultaneously.

In this study, a hybrid evolutionary method is proposed which, according to Eiben and Smith [14], belongs to the class of Memetic Algorithms [15]. These algorithms use problem-specific information to circumvent the No Free Lunch theorem [16] which states that, on average, all non-revisiting black box algorithms exhibit the same performance over the space of all possible problems. Thus, taking advantage of inherent problem characteristics, it is possible to devise an algorithm with significantly above-average performance [14].

The structure of the proposed method is threefold. First, a GA variant is employed which rapidly explores the search space, leading towards promising regions. In the next phase, a hill-climbing technique handles the exploitation of solutions by providing local optima. Finally, the feasible domain of parameters is subjected to a contraction operation which guides the algorithm in a convergent path towards optimality. This process allows for more accurate results [11] and has been streamlined using weight, truncation and coefficient control which is based on the progress of identification.

When employed for the identification of Bouc–Wen hysteretic systems, the method is proved to be efficient, robust and insensitive to noise-corrupted data; it can also identify viscous-type damping based on suitable experiments. Its performance is tested with a real experiment representing a full-scale steel cantilever beam which is identified successfully. Finally, a series of parametric studies are conducted that justify and demonstrate the role of each constituent component of the proposed method.

2. Model formulation

The equation of motion of a single-degree-of-freedom (sdof) system is expressed as

$$m\ddot{u}(t) + c\dot{u}(t) + F(t) = f(t), \tag{1}$$

where m is the mass, $u(t)$ is the displacement, c the linear viscous damping coefficient, $F(t)$ the restoring force and $f(t)$ the excitation force while the overdot denotes the derivative with respect to time. According to the Bouc–Wen model, the restoring force is expressed as

$$F(t) = a\frac{F_y}{u_y}u(t) + (1-a)F_y z(t), \tag{2}$$

where F_y is the yield force, u_y the yield displacement, a the ratio of post-yield to pre-yield (elastic) stiffness and $z(t)$ a dimensionless hysteretic parameter that obeys the following nonlinear differential equation with zero initial condition ($z(0) = 0$):

$$\dot{z}(t) = \frac{1}{u_y}[A - |z(t)|^n(\beta + sgn(\dot{u}(t)z(t))\gamma)]\dot{u}(t), \tag{3}$$

where, A, β, γ and n are dimensionless quantities controlling the behavior of the model and $sgn(\cdot)$ is the signum function. For small values of the positive exponential parameter n the transition from elastic to post-elastic branch is smooth, whereas for large values the transition becomes abrupt, approaching that of a bilinear model. Parameters β and γ control the size and shape of the hysteretic loop. Parameter A was introduced into the original formulation of the Bouc–Wen model, but recently it became evident that it is redundant [17].

From Eq. (2) it follows that the restoring force $F(t)$ can be divided into an elastic and a hysteretic part as follows:

$$F^{el}(t) = a\frac{F_y}{u_y}u(t), \tag{4}$$

$$F^{h}(t) = (1-a)F_y z(t). \tag{5}$$

Thus, the model can be visualized as two springs connected in parallel (Fig. 1) where, $k_i = F_y/u_y$ and $k_f = ak_i$ are the initial and post-yielding stiffness of the system.

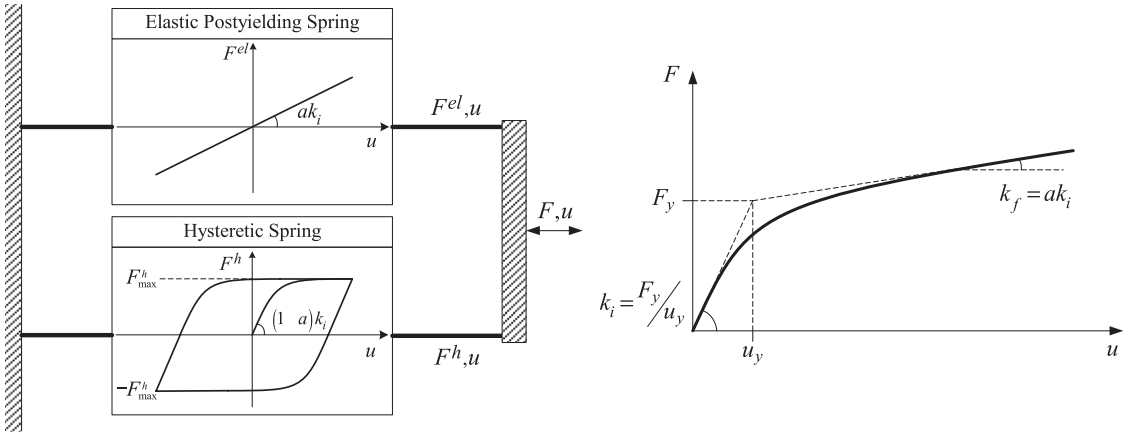

Fig. 1. Bouc–Wen model.

In displacement-controlled experiments, the time history of the displacement and its derivatives are readily available. Thus, the calculation of the hysteretic variable and restoring force is performed directly using Eqs. (3) and (2), respectively. In case of force-controlled experiments, by substituting Eq. (2) into Eq. (1) one obtains:

$$m\ddot{u}(t) + c\dot{u}(t) + a\frac{F_y}{u_y}u(t) + (1-a)F_y z(t) = f(t). \tag{6}$$

Eqs. (6) and (3) are written in state-space form and solved by any efficacious first-order differential equation solver, e.g. the Livermore "predictor–corrector" method [18], the Rosenbrock method [19] or the simple 4th–5th-order Runge–Kutta method. The latter is more efficient in terms of computational time and thus more suitable for stochastic optimization algorithms; the other methods are more accurate and were employed for verification purposes.

3. Parameter constraints

Recently, it was proved [17] that the parameters of the Bouc–Wen model are functionally redundant, i.e. there exist multiple parameter vectors that produce an identical response for a given excitation. Removing this redundancy is best achieved by fixing parameter A to unity [17].

Furthermore, parameters β and γ control the form of hysteretic loops, as demonstrated by Wen [2]. However, these parameters do not have clear physical meaning and affect the entire behavior in an indirect way. Early studies by Constantinou and Adnane [20] suggested imposing a certain constraint, viz. $A/(\beta+\gamma) = 1$, in order to reduce the model to a formulation with well-defined properties.

Adopting the aforementioned constraints, the total number of unknown parameters is reduced to six, i.e. γ, n, a, F_y, u_y and c. Additional parameters are required in cases when non-symmetric behavior or degradation phenomena are taken into account.

4. Identification scheme

4.1. Objective function and optimization problem

In this study, the normalized mean square error (MSE) of the predicted time history $\hat{y}(t|\mathbf{p})$ as compared to the reference time history $y(t)$ is used as an objective function. When cast in discrete form, it can be expressed as

$$\mathrm{OF}(\mathbf{p}) = \frac{\sum_{i=1}^{N}(y(t_i) - \hat{y}(t_i|\mathbf{p}))^2}{N\sigma_y^2}, \tag{7}$$

where $\mathbf{p}$ is the parameter vector, σ_y^2 the variance of the reference time history and N the number of points used. The time history of the displacement and external force is used for force- and displacement-controlled experiments, respectively.

Formally, the optimization problem can be stated as the minimization of the objective function when the parameter vector is subjected to the following side constraints:

$$\mathbf{p}_{\min} \leqslant \mathbf{p} \leqslant \mathbf{p}_{\max}, \tag{8}$$

where $\mathbf{p}_{\min}$ and $\mathbf{p}_{\max}$ are vectors defining the lower and upper bounds of model parameters, respectively.

4.2. Evolutionary algorithm

Evolutionary Algorithms (EAs), which are inspired by natural selection and survival of the fittest, are widely used for global optimization. For real-valued continuous-space functions, many researchers opt for real-coded EAs, e.g. Differential Evolution [21] or Particle Swarm Optimization [22]. In these cases, although mapping between genotype and phenotype is convenient, special operators must be devised to account for processes such as crossover, mutation, recombination, generation of valid trial vectors, etc. On the other hand, common bit-coded GAs can accommodate a local optimizer very easily. Hybrid EAs outperform both its constituents for a broad spectrum of practical applications [14] which also holds for the method presented herein.

Thus, in this study, the Hybrid EA is composed of Sawtooth GA [23] and Greedy Ascent Hill Climbing (GAHC) to local optimality [14]. Sawtooth GA was introduced recently and uses variable population size and partial reinitialization in a synergistic way to enhance performance. It displays good performance when compared to Standard-GA and other GAs that use reinitialization of the population, such as the micro-GA, suggested by Goldberg [24] and first implemented by Krishnakumar [25]. According to Sawtooth GA, the population size follows a predefined scheme (Fig. 2) which is characterized by mean population N_m, amplitude of variation $D < N_m$ and period T. From parametric studies with a large test bed of unimodal and multimodal problems, it became evident that strong reinitialization of the population, i.e. large values of D/N_m, is beneficial.

A single-point crossover scheme with probability 0.7 is adopted. The mutation scheme includes jump mutation with probability $1/P$ and creep mutation with probability $L_c/N_p/P$, where P is the current population size, L_c the chromosome length and N_p is the number of unknown parameters.

After a specific number of generations, the best individual produced by Sawtooth GA becomes the seed for GAHC. This solution is improved by continuously flipping the bits of the chromosome from left to right, keeping the best result as a reference. When a full cycle of bit flips has been concluded without improvement, the local optimum has been found [14].

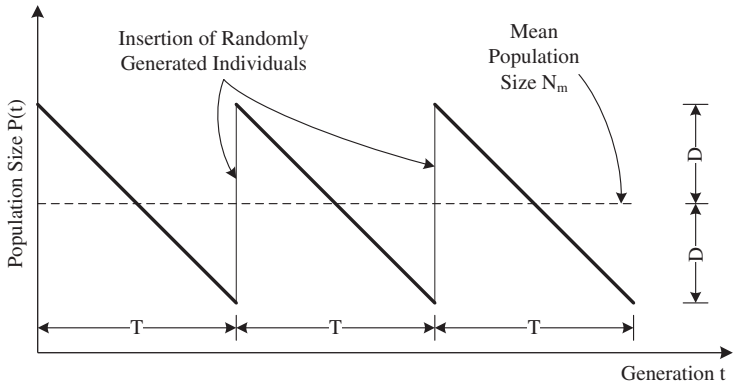

Fig. 2. Sawtooth population variation scheme.

4.3. Bounding

At each optimization step j, the hybrid EA is applied for M_r independent runs of a few generations each. These runs can be performed in parallel within a computer network, thus reducing the computing time drastically. The solutions are sorted and the worse M_t ones are truncated. Considering the remaining $M_r - M_t$ solutions, weighting coefficients are assigned as follows:

$$w_k = \frac{\max_k(\mathrm{OF}_k)}{\mathrm{OF}_k}, \tag{9}$$

where OF_k is the objective function value of the kth solution. According to the above formulation, the worst solution is assigned a weight of unity. The weighted mean value of parameter i is calculated as follows:

$$m_i = \frac{\sum_{k=1}^{M_r-M_t}(w_k p_{ik})}{\sum_{k=1}^{M_r-M_t}(w_k)}, \tag{10}$$

where p_{ik} is the value of parameter i of the kth solution. The descriptive weighted standard deviation is expressed as

$$s_i = \sqrt{\frac{\sum_{k=1}^{M_r-M_t}(w_k(p_{ik}-m_i)^2)}{\sum_{k=1}^{M_r-M_t}(w_k)}}. \tag{11}$$

The new trial upper and lower bounds of parameter i are defined symmetrically around the weighted mean value m_i as follows:

$$\overline{u}_{i,j+1} = m_i + qs_i,$$

$$\overline{l}_{i,j+1} = m_i - qs_i, \tag{12}$$

where q is a real coefficient which represents the semi-width of the new trial range in terms of standard deviation. Finally, the feasible domain of parameter i in the next optimization step is defined as the intersection of the current range with the trial range:

$$[l_{i,j+1}, u_{i,j+1}] = [l_{ij}, u_{ij}] \cap [\overline{l}_{i,j+1}, \overline{u}_{i,j+1}]. \tag{13}$$

It is noted that, based on Eq. (13), the feasible domain is not allowed to expand. If a specific parameter is insensitive then the results will be scattered almost uniformly. Provided that the statistical sample is sufficient, the standard deviation s_i will be significant and the range will remain unaffected. Thus, instead of being trapped into local optima, the contraction process is suspended on a parameter basis when statistical analysis of the results does not justify progress. It is observed that sensitive parameters are identified faster and assist insensitive ones in subsequent steps. Thus, a measure of relative parameter sensitivity is revealed by the identification process.

Another important feature is that the proposed method is safe when the optimum parameter value lies at one end of the range. This is because, in general, the weighted mean value will lie close to the same end. Since the new trial range is formed symmetrically around this value, the optimum will remain within the search space.

4.4. Coefficient control and termination

A linear variation rule that controls the coefficients of the proposed algorithm is introduced. Considering parameter i, the ratio of the range at current step j to the initial range is employed as a progress indicator:

$$a_{ij} = \frac{u_{ij} - l_{ij}}{U_i - L_i}, \tag{14}$$

where u_{ij} and l_{ij} are the upper and lower bounds at step j and U_i, L_i are the initial upper and lower bounds, respectively. The range ratio has an initial value equal to unity and decreases as identification progresses. The variation is controlled by the range ratio a_j of the parameter that has progressed the least, i.e. $a_j = \max_i\{a_{ij}\}$.

When considering real coefficients, the rule is expressed as

$$r = \begin{cases} r_e + (r_s - r_e)\left(\dfrac{a_j - a_{r1}}{1 - a_{r1}}\right), & a_{r1} \leqslant a_j \leqslant 1, \\ r_e, & a_j < a_{r1}, \end{cases} \tag{15}$$

where r_s and r_e are the initial and final values of the coefficient, respectively. Parameter a_{r1}, with a typical value of 1.0×10^{-3}, is the range ratio that signifies that identification has practically concluded. In this study, the overall stop criterion is a_j reaching the threshold of 1.0×10^{-4}. At this point, the upper and lower bound of all model parameters practically coincide.

5. Identification

The efficiency of any identification scheme depends heavily on the information contained in the input–output data. These should encapsulate all system features and characteristics that need to be identified. The relative performance of the proposed method with respect to various levels of informational input and the occasional presence of viscous damping is investigated.

It was observed that identification of hysteretic, i.e. rate-independent damping can be performed with a simple periodic excitation of few cycles; in this case, viscous damping is either neglected or considered known. Three cases of 3-period displacement-controlled sinusoidal experiments are considered, namely cases 1a to 1c (Fig. 3). The amplitude is equal to 0.5, 2.0 and 7.0 times the yield displacement, respectively. In addition, the response under the El Centro excitation is considered with an oscillating mass equal to $28.6\,\mathrm{kNs^2/m}$ and peak ground acceleration (PGA) equal to $0.319g$, which results in a maximum displacement almost equal to $2.0u_y$ (case 1d). The true parameter values, initial side constraints and the mean results of ten independent runs are summarized in Table 1, while the comparative performance is shown in Fig. 4. These analyses were performed using the following algorithm settings: number of runs $M_r = 40$, number of discarded runs $M_t = 10$, standard deviation coefficient $q = 3.0$, mean population size $N_m = 25$, amplitude of variation $D = 20$ and period $T = 5$.

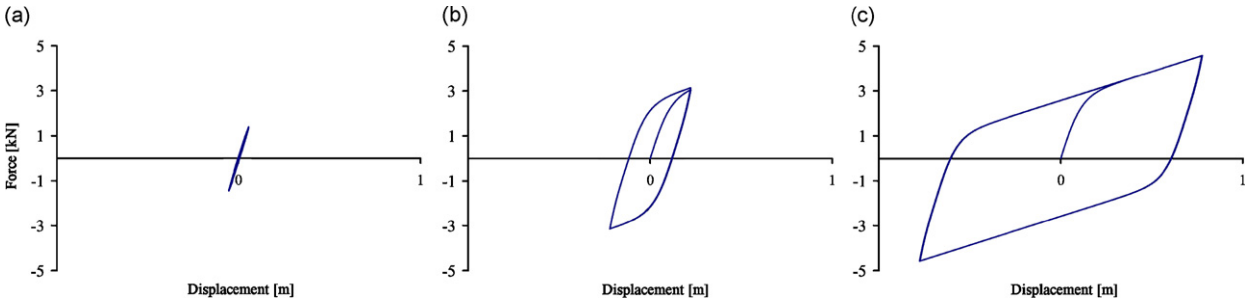

Fig. 3. Hysteretic loops for sinusoidal displacement with $u_{\max}/u_y$ equal to: (a) 0.5, (b) 2.0, (c) 7.0.

Table 1
True values, initial side constraints and final results with viscous damping known

	γ	n	a	F_y (kN)	u_y (m)	c (kNs/m)
True value	0.9000	2.0000	0.1000	2.8600	0.1110	0.0000
Initial lower bound	0.0000	1.0000	0.0000	0.1000	0.0100	–
Initial upper bound	1.0000	10.0000	1.0000	10.0000	1.0000	–
1a ($u_{\max} = 0.5u_y$)	0.8856	1.9562	0.1075	2.8987	0.1123	–
1b ($u_{\max} = 2.0u_y$)	0.8991	1.9986	0.1000	2.8597	0.1110	–
1c ($u_{\max} = 7.0u_y$)	0.8676	1.9220	0.0987	2.8552	0.1093	–
1d (El Centro)	0.9000	2.0000	0.1000	2.8600	0.1110	–

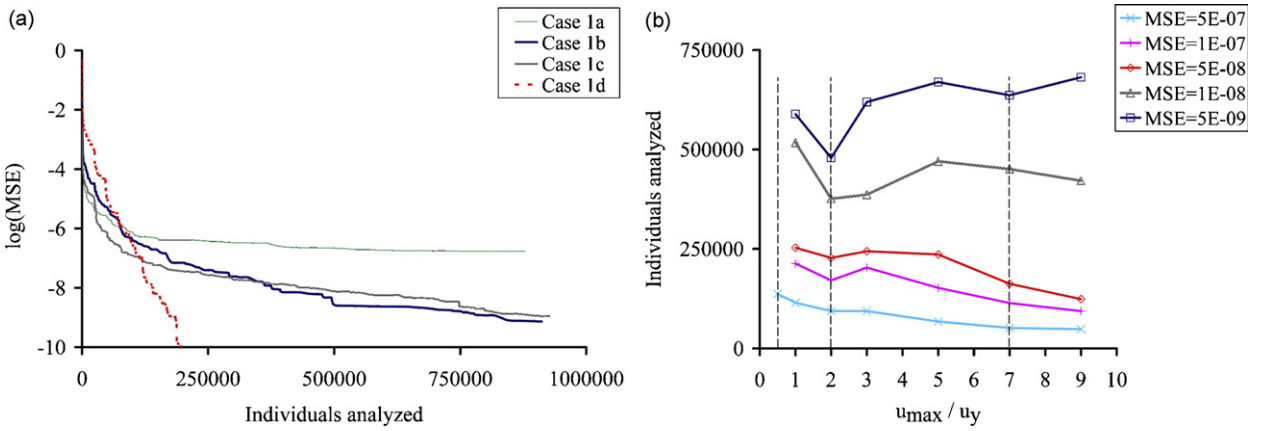

Fig. 4. Comparative performance with viscous damping known.

Table 2
True values, initial side constraints and final results with viscous damping unknown

	γ	n	a	F_y (kN)	u_y (m)	c (kNs/m)
True value	0.9000	2.0000	0.1000	2.8600	0.1110	5.4292
Initial lower bound	0.0000	1.0000	0.0000	0.1000	0.0100	0.0000
Initial upper bound	1.0000	10.0000	1.0000	10.0000	1.0000	100.0000
2a ($u_{\max} = 2u_y$)	0.6211	1.5397	0.1736	2.5542	0.1013	6.4835
2b ($u_{\max} = 2u_y, 7u_y$)	0.9000	2.0000	0.1000	2.8600	0.1110	5.4292
2c (El Centro)	0.9000	2.0000	0.1000	2.8600	0.1110	5.4292

Sawtooth GA was allowed to evolve for 15 generations ($K_T = 3$) and 10 bits were allocated for each unknown parameter ($L_g = 10$).

In the case of El Centro excitation (case 1d) "exact" parameter values, i.e. to four decimal digits, are readily obtained. For the cases of sinusoidal displacement, the first response is almost linear and does not contain information on the post-elastic regime; as a result, identification fails to progress (Fig. 4a). In case 1c, the response is strongly nonlinear and the best initial performance is observed (Fig. 4a,b). This is because most of the information refers to the post-elastic regime and the corresponding bilinear backbone is identified quickly. For the opposite reason, however, the sensitivity of the parameters controlling the transition between branches is small. In the proposed method, the stop criterion is based on narrowing of parameter ranges rather than reaching an MSE threshold. Thus, the best overall performance is exhibited by case 1b, in which the system just enters the post-elastic region and the sensitivity of all parameters is of comparable magnitude (Fig. 4a,b).

When viscous damping is unknown, identification with a single sinusoidal experiment occasionally fails by predicting values of viscous damping coefficient greater than the true ones. This is because, under simple harmonic excitation, damping is more easily attributed to the linear viscous damping term. Moreover, the rate-dependent viscous damping is strongly dependent on amplitude [26]. Therefore, this problem can be readily addressed by combining two experiments of different amplitude and/or frequency, e.g. cases 1b and 1c. In this case, the mean normalized MSE is used as an objective function and identification with unknown viscous damping is always successful. In illustration, three cases are considered, namely cases 2a–2c. These are, respectively, a failed attempt using experiment 1b only, a combination of cases 1b and 1c and the response under the El Centro excitation. The true parameter values, initial side constraints and identification results are summarized in Table 2. The viscous damping coefficient equals 10% of the critical value. The hysteretic loop of case 2a, as compared to the true system response, is shown in Fig. 5a. "Exact" parameter values, i.e. to four decimal digits, are obtained for both cases 2b and 2c; however, the combination of two sinusoidal experiments exhibits roughly three times better performance (Fig. 5b).

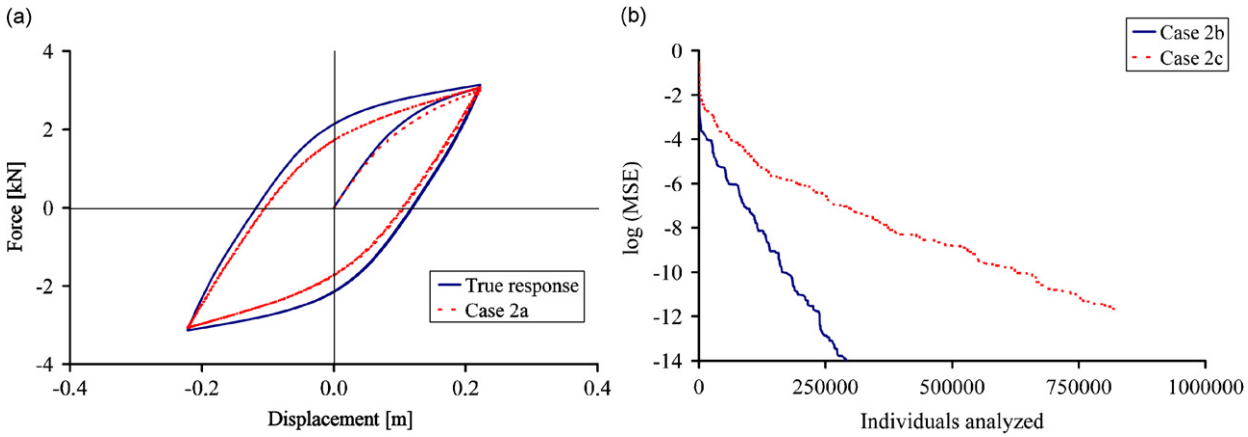

Fig. 5. (a) Case 2a as compared to true response; (b) performance comparison of cases 2b and 2c.

Table 3
Identification results from noise-corrupted data

	γ	n	a	F_y (kN)	u_y (m)	c (kNs/m)
3a (NSR = 1%)	0.9010	1.9998	0.1000	2.8608	0.1110	5.4261
3b (NSR = 5%)	0.9019	2.0096	0.1001	2.8569	0.1110	5.4369
3c (NSR = 10%)	0.8993	1.9953	0.0995	2.8642	0.1111	5.4014

6. Noise

Experimental data are always corrupted by noise that is introduced during measurement. The proposed scheme was used to identify hysteretic systems with simulated noisy data that are produced in the following manner:

$$\bar{y}(t_i) = (1 + \varepsilon r_i) y(t_i), \tag{16}$$

where r_i's are a sequence of random variables with a uniform distribution in the interval $(-1, 1)$ and parameter ε is the noise to signal ratio (NSR). Three cases were considered, namely cases 3a to 3c, with NSR equal to 1%, 5% and 10%, respectively. The El Centro excitation and an oscillating mass equal to $28.6\,\mathrm{kNs^2/m}$ were used. The true parameter values and initial side constraints are given in Table 2. No noise pre-filtering was applied.

The results, summarized in Table 3, demonstrate that the proposed scheme is insensitive to noise. The Bounding progress of the most insensitive parameter, i.e. parameter γ, is shown in Fig. 6. It is observed that faster convergence occurs for lower levels of noise contamination.

7. Identification using real data

The proposed method was used to identify a hysteretic system representing a full-scale steel cantilever beam. The experiment, namely experiment No. 5, was conducted by Popov and Stephen [27] at Berkeley in 1970 and refers to a WF 24 × 76 beam (A36 Grade) that was connected to a rigid column. The flanges were welded to the column, while the web was bolted using seven 7/8″ bolts (Fig. 7a). The free end of the beam was subjected to a quasi-static cyclic displacement pattern. The response exhibited clear non-degrading hysteretic behavior.

The initial side constraints and the identified values are summarized in Table 4. It is noted that no effort has been made to pre-estimate the actual values. In particular, the side constraints of parameters F_y and u_y were selected with a simple inspection of the force–displacement diagram. Using an even wider range would scarcely encumber the progress of identification, as the extreme values are readily discarded during the initial stages.

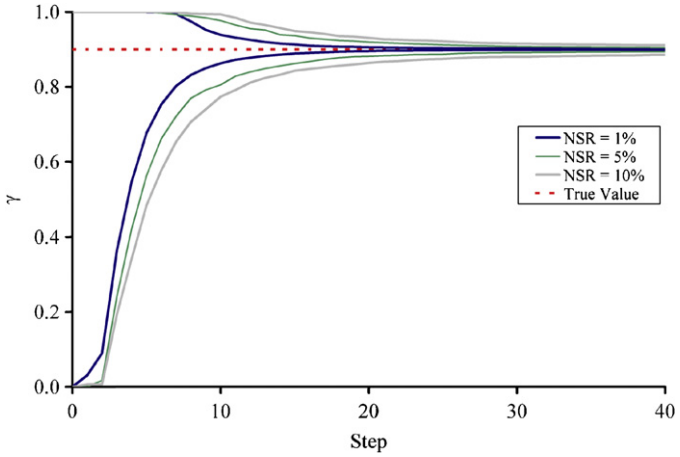

Fig. 6. Bounding progress of parameter γ with noise-corrupted data.

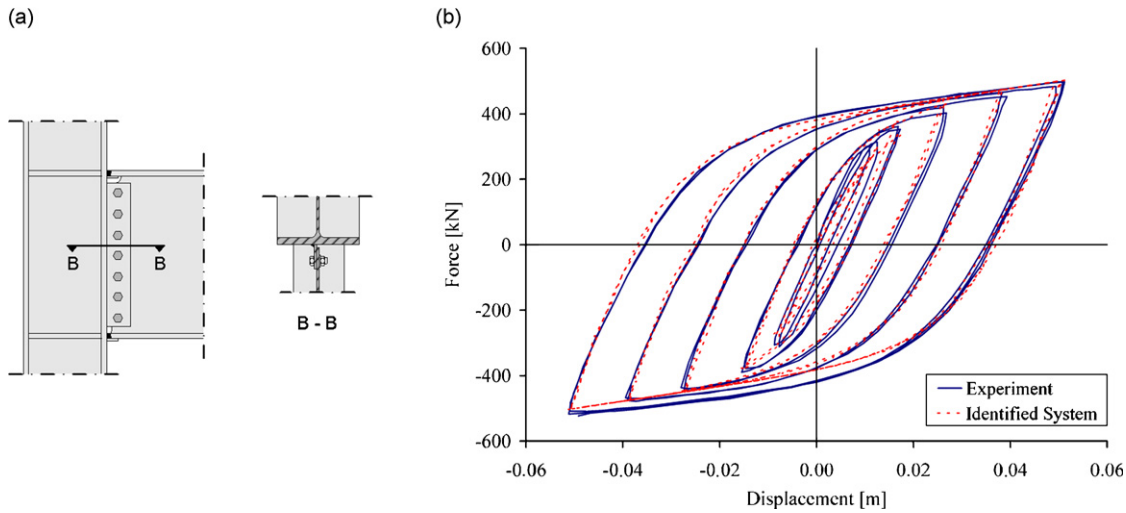

Fig. 7. (a) Bolted-welded connection, (b) force–displacement diagram.

Table 4
Initial side constraints and identified parameter values (cantilever beam)

	γ	n	a	F_y (kN)	u_y (m)
Initial lower bound	0.0000	1.0000	0.0000	0.0000	0.0010
Initial upper bound	1.0000	10.0000	1.0000	1000.0000	0.1000
Identified value	1.0000	1.3248	0.0756	420.2587	0.0142

The response of the identified system is in good agreement with experimental data (Fig. 7b). As an indication of the robustness of the proposed method, it is noted that several independent runs were executed and the final results were almost identical. The final value of normalized MSE was 0.51%; however, a value of 0.59% was already achieved after 5000 function evaluations. It is also noted that the experimental data are

slightly asymmetric; this feature cannot be handled by the symmetric Bouc–Wen model that is considered herein.

8. Parametric studies

A series of parametric studies have been conducted that reveal the inner workings of the proposed scheme. For each case, the configuration of the hybrid EA and Bounding are summarized in Tables 5 and 6, respectively. In case of varying coefficients, both the start and the end values are given, separated by a slash. The El Centro excitation and an oscillating mass equal to $28.6\,\mathrm{kNs^2/m}$ were used. The viscous damping coefficient equals 10% of the critical value and is considered unknown. The true parameter values and initial side constraints are given in Table 2.

For comparison purposes, the mean progress of the best individual was calculated based on ten independent runs. Efficiency is measured by the number of function evaluations required for a specific level of normalized MSE. The actual results are not shown, since a normalized MSE around 10^{-10} invariably means that all parameters have been identified "exactly", i.e. to four decimal digits.

Cases A1–A4 (Fig. 8a) reveal the effect of Sawtooth period T in the overall performance. Although values of T/N_m around 0.50 are suggested [23], in this study using even smaller periods is beneficial. This indicates that

Table 5
Parameters of hybrid EA: N_m is the mean population, D the amplitude of variation, T the period, K_T the number of applied periods per run and L_g the gene length

Case	N_m	D	T	K_T	L_g	GAHC
A1	25	20	5	3	10	Yes
A2	25	20	10	3	10	Yes
A3	25	20	15	3	10	Yes
A4	25	20	20	3	10	Yes
B1	15	12	5	5	10	Yes
B4	15	12	20	5	10	Yes
C1	25	20	5	2	10	Yes
C2	25	20	5	4	10	Yes
D1	25	20	5	3	8	Yes
D2	25	20	5	3	15	Yes
D3	25	20	5	3	15/10	Yes
E1	25	20	5	3	10	No
E2	25	20	5	5	10	No
F–H	25	20	5	3	10	Yes

Table 6
Parameters of Bounding: M_r is the number of runs, M_t the number of truncated runs and q the standard deviation coefficient

Case	M_r	M_t	q
A–E	40	10	3.0
F1	30	0	3.0
F2	35	5	3.0
G1	40	10	3.0/2.5
G2	40	10	3.0/2.0
H1	30	8	3.0
H2	20	5	3.0

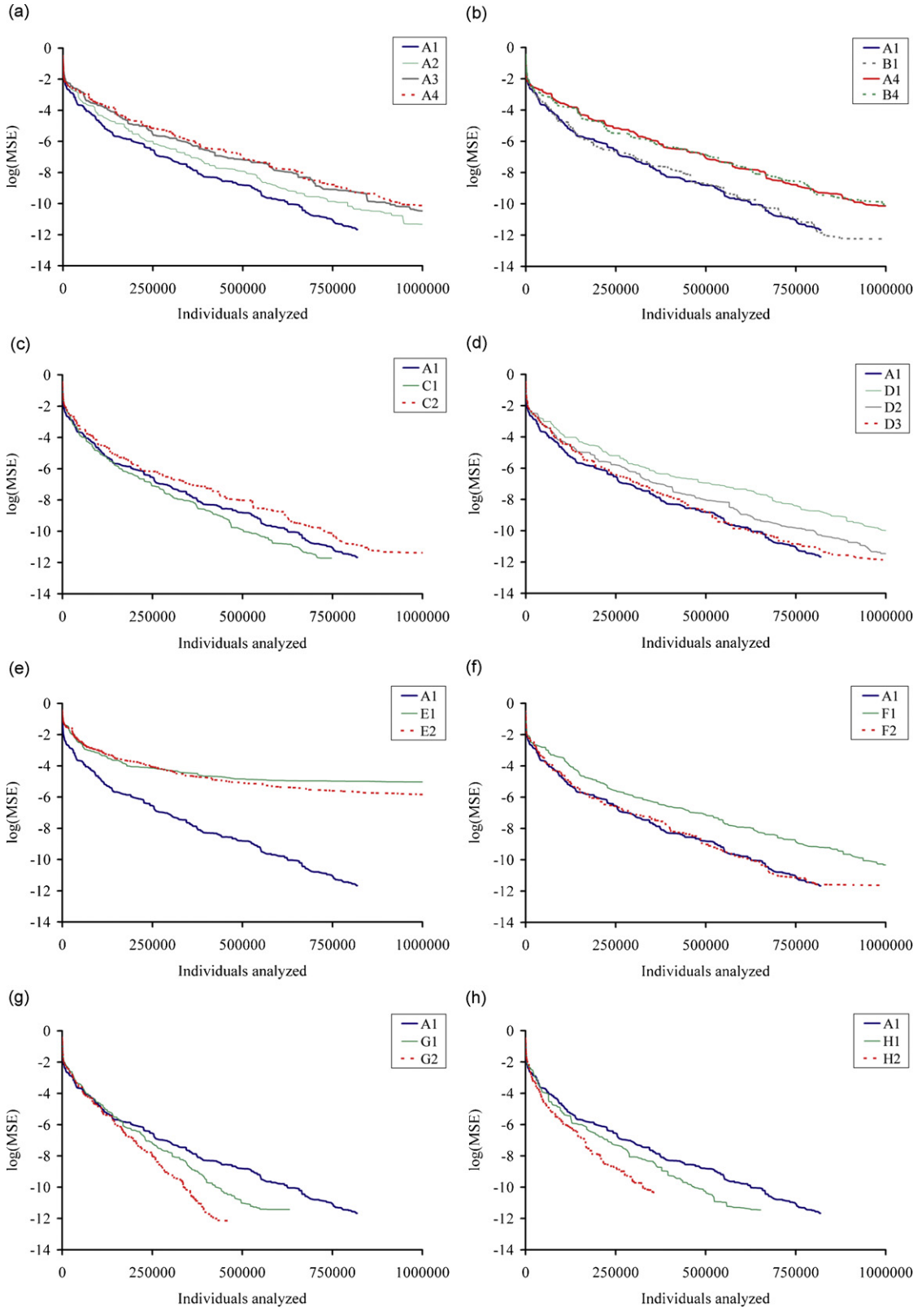

Fig. 8. Parametric study corresponding to Tables 5 and 6.

reinitialization rather than recombination is the main driving force of the GA, which can be attributed to the coarse discretization of the search space.

Cases B1 and B4, as compared to A1 and A4, respectively, show that different combinations of mean population N_m and number of Sawtooth periods K_T produce similar results. In illustration, cases A1 and B1 both include 375 analyses while 125 and 123 random individuals are introduced per run, respectively. As a result, their mean progress is similar (Fig. 8b).

For a constant mean population equal to 25 individuals, cases C1 and C2 indicate that few Sawtooth periods are sufficient to produce a good seed for GAHC (Fig. 8c).

Cases D1–D3 (Fig. 8d) reveal the effect of the chromosome length in the overall efficiency. It is shown that too small or too large a chromosome length leads to reduced performance; the former can be attributed to insufficient discretization of the search space (case D1), the latter to the increased number of analyses required by GAHC to provide the local optimum (case D2). Using variable chromosome length that accounts for the narrowing of the range does not seem to provide an advantage (case D3).

Cases E1 and E2 (Fig. 8e) reveal the decisive role of GAHC in the overall performance. Case E1 is identical to reference case A1 without GAHC, whereas case E2 features two additional Sawtooth periods that roughly compensate for the mean number of individuals analyzed by GAHC.

Cases F1 and F2 (Fig. 8f) demonstrate the beneficial effect of truncation. It is shown that even when few results are truncated (case F2), the performance is increased significantly.

One of the most important factors is coefficient q which governs the size of the trial feasible domain of parameters. As identification progresses, the standard deviation s_i becomes comparable to the narrowed range of values. Thus, it is preferable to use a safe value of q at the beginning, so as to ensure that optimum values remain within the search space, and decrease it gradually to accelerate convergence. This is demonstrated in cases G1 and G2 (Fig. 8g), in which the final value of q is equal to 2.5 and 2.0, respectively.

Finally, the efficiency of the scheme is directly related to the sample size M_r. This is demonstrated in cases H1 and H2 (Fig. 8h), in which the total sample size is reduced to 30 and 20 runs, respectively.

All analyses presented herein converged safely to the true values; however, it is obvious that small values of q or insufficient sample size M_r may lead to failure. Clearly, this depends on the excitation and the initial side constraints. Although a limited set of data is presented, many experiments have been conducted that support the observations made herein. Earlier studies by the authors [28] suggest that sdof systems with various periods and viscous damping are also identifiable. The efficiency of identification is related to the shape and size of hysteretic loops rather than to individual system properties or excitation characteristics.

9. Comparison with standard GA and micro-GA

A series of comparative analyses were conducted to demonstrate the improved performance of the proposed scheme as compared to Standard GA and micro-GA. The hysteretic system representing the cantilever beam was identified using Standard GA with $P = 25$ and 50. Similar settings were used, i.e. $L_c = 50$ ($L_g = 10$ bits per unknown parameter), single-point crossover with probability 0.7, elitism, jump mutation with probability $1/P$ and creep mutation with probability $L_c/N_p/P$. In addition, micro-GA was employed with $P = 5$ and single-point crossover. The mean performance of 30 independent runs shows that the proposed method outperforms both Standard GA and micro-GA for the specific problem (Fig. 9).

In terms of identification accuracy, the proposed method is more efficient because the chromosomes, with either fixed or variable length, refer to a constantly contracting search space. Hence, increased accuracy to a desired level is feasible which is verified using simulated experiments. This is not possible either in Standard GA or micro-GA due to fixed discretization of the search space.

10. Suggested algorithm settings

The parameters used with case A1 can be considered conservative and safe for most applications of similar complexity. This configuration was used with the main identification experiments. Cases G2 and H2 exhibit improved performance and were used with the noise-corrupted data and the cantilever beam, respectively.

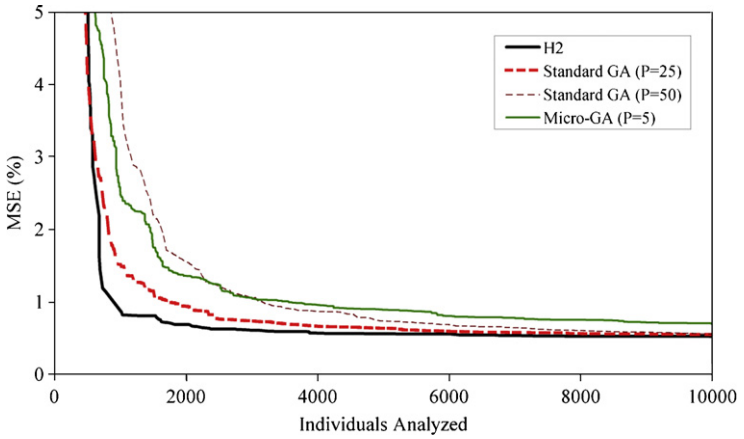

Fig. 9. Comparative performance of the proposed method, Standard GA and micro-GA.

For problems with more unknown variables, both the exploration and the sampling of the search space should be more intensive. Suggested algorithm settings are as follows: the mean population size N_m of Sawtooth GA equals 30–50% of L_c. The amplitude of variation D is chosen so that $N_m - D$ equals 1 to 5. For a moderate number of unknown parameters, the number M_r of independent runs is of the order of N_p^2 at most, while the number M_t of truncated runs equals 5–20% of M_r. All other parameters can be chosen based on the conclusions of the parametric studies presented herein. However, every problem exhibits its own intrinsic characteristics and preliminary experimentation with the algorithm settings is required.

11. Conclusions

A new stochastic identification method is presented. The scheme consists of a recently introduced GA variant, namely Sawtooth GA [23]; a local optimizer, namely Greedy Ascent Hill Climbing (GAHC) [14]; and a Bounding process developed herein. It is shown that the proposed method is efficient and robust in identifying Bouc–Wen hysteretic systems using noise-free or noise-corrupted data. As typical of evolutionary algorithms, the proposed method is gradient-free and lends itself to massive parallel computing. In addition, it can accommodate other evolutionary and/or heuristic methods due to its modular structure.

When compared to Standard GA and micro-GA, the proposed method exhibited enhanced performance for the problems of this investigation. Sawtooth GA is responsible for the rapid exploration of the search space, while GAHC handles the exploitation of solutions. Rather than allowing the inevitable performance degradation, which is typical of EAs [14], the proposed method uses solely the initial explosive phase of evolution. The Bounding process specifies a single range of values per gene, which represents a single-valued model parameter with an unambiguous physical interpretation. This process is not affected by the variability in parameter sensitivity that is commonly experienced with the Bouc–Wen model.

It is emphasized that valuable conclusions can be drawn from the progress of Bounding. Although very good individuals, in terms of fitness, may occasionally be discovered, insufficient progress in terms of Bounding is a clear indication that system identification is inconclusive. This can be attributed to either deficiencies of the model, e.g. use of redundant, multi-valued or constantly insensitive parameters or inappropriate experiment design. This behavior was consistently observed in several cases, as for example when allowing the redundant parameter A to vary, or when using an almost linear experiment to identify parameters governing nonlinear response.

In general, the proposed method is not particularly sensitive to the selection of its parameters as demonstrated by the parametric studies. Moreover, guidelines on the proper selection of parameters are provided herein.

Although there is no identification method that can be characterized as panacea, the proposed scheme exhibits enhanced performance due to its adaptive features.

Acknowledgments

This work has been funded by the project PENED 2003. The project is co-financed 75% of public expenditure through EC—European Social Fund, 25% of public expenditure through Ministry of Development—General Secretariat of Research and Technology and through private sector, under measure 8.3 of Operational Programme "Competitiveness" in the 3rd Community Support Programme.

References

[1] R. Bouc, Forced vibration of mechanical systems with hysteresis, *Proceedings of the Fourth Conference on Non-linear Oscillation*, Prague, Czechoslovakia, 1967.
[2] Y.K. Wen, Method for random vibration of hysteretic systems, *ASCE Journal of Engineering Mechanics Division* 102 (EM2) (1976) 249–263.
[3] M. Yar, J.K. Hammond, Parameter estimation for hysteretic systems, *Journal of Sound and Vibration* 117 (1) (1987) 161–172.
[4] S.K. Kunnath, J.B. Mander, L. Fang, Parameter identification for degrading and pinched hysteretic structural concrete systems, *Engineering Structures* 19 (3) (1997) 224–232.
[5] R.H. Sues, S.T. Mau, Y. Wen, System identification of degrading hysteretic restoring forces, *Journal of Engineering Mechanics* 114 (5) (1988) 833–846.
[6] H. Zhang, G.C. Foliente, Y. Yang, F. Ma, Parameter identification of inelastic structures under dynamic loads, *Earthquake Engineering and Structural Dynamics* 31 (2002) 1113–1130.
[7] Y.Q. Ni, J.M. Ko, C.W. Wong, Identification of non-linear hysteretic isolators from periodic vibration tests, *Journal of Sound and Vibration* 217 (4) (1998) 737–756.
[8] J.-S. Lin, Y. Zhang, Nonlinear structural identification using extended Kalman filter, *Computers and Structures* 52 (4) (1994) 757–764.
[9] N.M. Kwok, Q.P. Ha, M.T. Nguyen, J. Li, B. Samali, Bouc–Wen model parameter identification for a MR fluid damper using computationally efficient GA, *ISA Transactions* 46 (2007) 167–179.
[10] J.-L. Ha, Y.-S. Kung, R.-F. Fung, S.-C. Hsien, A comparison of fitness functions for the identification of a piezoelectric hysteretic actuator based on the real-coded genetic algorithm, *Sensors and Actuators A* 132 (2006) 643–650.
[11] A. Kyprianou, K. Worden, M. Panet, Identification of hysteretic systems using the differential evolution algorithm, *Journal of Sound and Vibration* 248 (2) (2001) 289–314.
[12] F. Ma, C.H. Ng, N. Ajavakom, On system identification and response prediction of degrading structures, *Structural Control and Health Monitoring* 13 (2006) 347–364.
[13] J.-L. Ha, R.-F. Fung, C.-S. Yang, Hysteresis identification and dynamic responses of the impact drive mechanism, *Journal of Sound and Vibration* 283 (2005) 943–956.
[14] A.E. Eiben, J.E. Smith, *Introduction to Evolutionary Algorithms*, Springer, Berlin, 2003.
[15] P.A. Moscato, On evolution, search, optimization, genetic algorithms and martial arts: towards memetic algorithms, Technical Report, Caltech Concurrent Computation Program Report 826, Caltech, Pasadena, California, 1989.
[16] D.H. Wolpert, W.G. Macready, No free lunch theorems for optimization, *IEEE Transactions on Evolutionary Computation* 1 (1) (1997) 67–82.
[17] F. Ma, H. Zhang, A. Bockstedte, G.C. Foliente, P. Paevere, Parameter analysis of the differential model of hysteresis, *Journal of Applied Mechanics ASME* 71 (2004) 342–349.
[18] C. Alan, ODEpack, a systemized collection of ODE solvers, in: R.S. Stepleman, et al. (Eds.), *Hindmarsh Scientific Computing*, North-Holland, Amsterdam, 1983.
[19] W.H. Press, S.A. Teukolsky, W.T. Vetterling, B.P. Flannery, *Numerical Recipes in C + +: the Art of Scientific Computing*, Cambridge University Press, Cambridge, 2002.
[20] M.C. Constantinou, M.A. Adnane, Dynamics of soil-base-isolated structure systems: evaluation of two models for yielding systems, Report to NSAF, Department of civil engineering, Drexel University, Philadelphia, PA, 1987.
[21] R. Storn, K. Price, Differential evolution—a simple and efficient heuristic for global optimization over continuous spaces, *Journal of Global Optimization* 11 (1997) 341–359.
[22] J. Kennedy, R.C. Eberhart, Particle swarm optimization, *Proceedings of IEEE International Conference on Neural Networks* IV (1995) 1942–1948.
[23] V.K. Koumousis, C.P. Katsaras, A saw-tooth genetic algorithm combining the effects of variable population size and reinitialization to enhance performance, *IEEE Transactions on Evolutionary Computation* 10 (1) (2006) 19–28.
[24] D.E. Goldberg, Sizing populations for serial and parallel genetic algorithms, *Proceedings of the Third International Conference on Genetic Algorithms (ICGA 89)*, 1989, pp. 70–79.
[25] K. Krishnakumar, Micro-genetic algorithms for stationary and nonstationary function optimization, *Proceedings of the SPIE Intelligent Control Adaptive Systems* (1989) 1942–1948.

[26] P.C. Jennings, Periodic response of a general yielding structure, *Journal of the Engineering Mechanics Division ASCE* 90 EM2 (1964) 131–166.
[27] E.P. Popov, R.M. Stephen, Cyclic Loading of Full-Size Steel Connections, UCB/EERC-70/03, 1970.
[28] A.E. Charalampakis, V.K. Koumousis, Parameter estimation of Bouc–Wen hysteretic systems using sawtooth genetic algorithm, *Proceedings of the Fifth International Conference on Engineering Computational Technology*, Las Palmas de Gran Canaria, Spain, 2006.